Geo.Alp, Vol. 13 2016 257 - 276

Field trip 12

Rock slope failures shaping the landscape in the Loisach-, Inn- and Ötz Valley region (Tyrol, Austria)

Marc Ostermann [1], Christoph Prager [2,3]

[1] Institute for Geology, University of Innsbruck, Innrain 52, 6020 Innsbruck, Austria

[2] alpS GmbH, Grabenweg 68, 6020 Innsbruck, Austria

[3] ILF Consulting Engineers Austria GmbH, Feldkreuzstraße 3, 6063 Rum bei Innsbruck, Austria

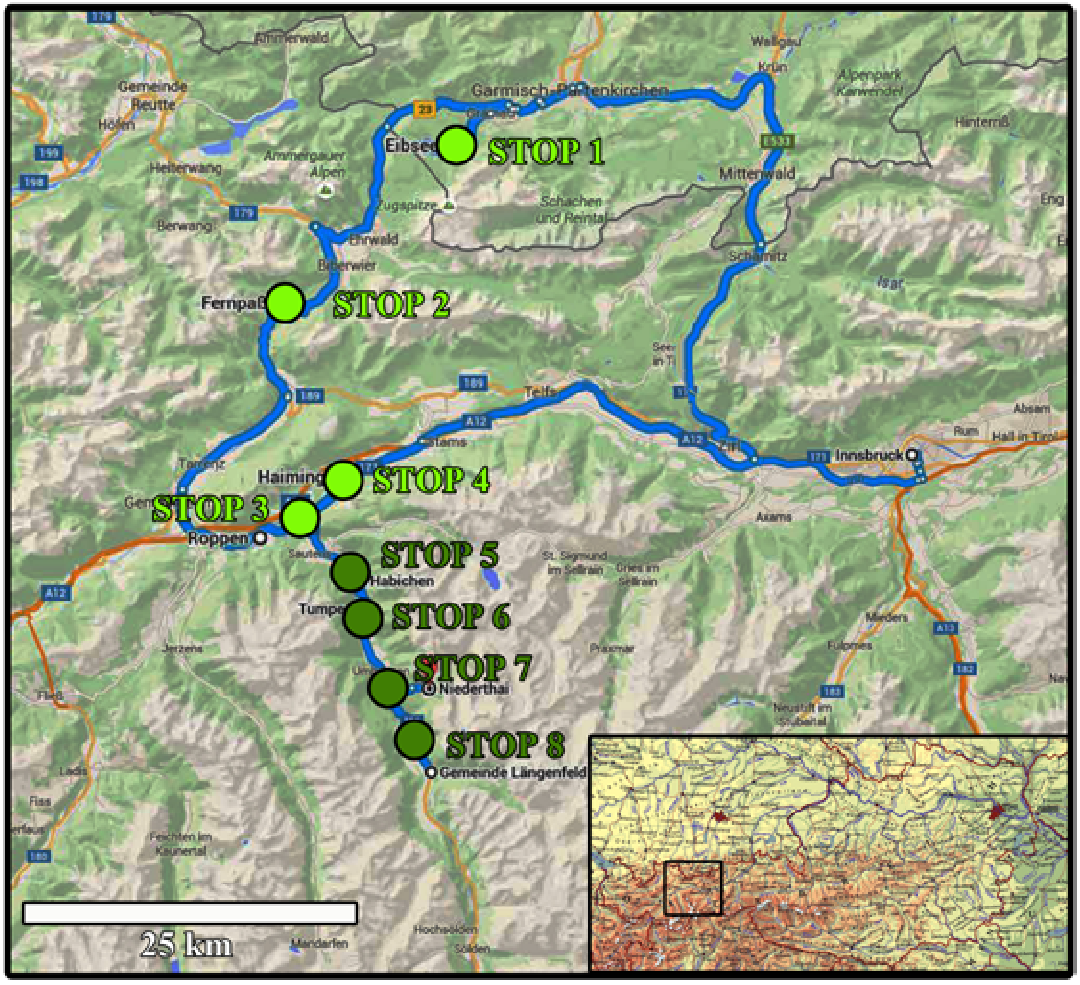

Fig. 1: Excursion route (blue line) starting in Innsbruck. The stops correspond to the numbering in the text. Stop 1: Eibsee rock avalanche; Stop 2: Fernpass rock avalanche; Stop 3: Tschirgant rock avalanche; Stop 4: Haiming rock avalanche; Stop 5: Habichen rock avalanche; Stop 6: Tumpen/Achplatte rock avalanche; Stops 7 & 8: Köfels rockslide.

Topics

Landscape shaping deposits of rock slope failures in the Loisach, Inn and Ötz valley region are prominent and intensively studied examples of Holocene mass wasting in Alpine environments. They feature various types of rockslides and rock avalanches with deposition volumes ranging between some 10- to some 100-million m^3 and runout distances extending up to several kilometres (e.g. Abele, 1974, Prager et al., 2008).
This excursion aims to provide compiled information from literature and new first-hand research data on the carbonate **rock avalanche deposits at Eibsee**, **Fernpass**, **Tschirgant** and **Haiming** (Loisach and Inn valley, day 1), and on the crystalline rock slope collapses at **Habichen**, **Tumpen** and **Köfels** (Ötz valley, day 2) (Fig. 1). New findings obtained from field surveys and remote sensing, dating, geophysical investigations and laboratory analyses e.g. on sedimentology and geochemistry are presented and discussed on-site. Additionally we address the major causes, mechanic behaviour, impact on the surroundings and secondary processes of the catastrophic bedrock failures in the region.

Geological Setting

The geological setting of the excursion area is characterised by two major tectono-stratigraphical units (Fig. 2), the **Northern Calcareous Alps (NCA)**, and the metamorphic **Öztal-Stubai-Basement (ÖSB).** These major nappe complexes are separated by the NE-striking **Upper Inn valley fault zone**, along which polyphase and heteroaxial brittle deformation occurred (Eisbacher & Brandner, 1995, Ortner, 2003).

The **Northern Calcareous Alps (NCA)** are a thin-skinned fold-and-thrust belt along the northern margin of the Austroalpine nappe pile (Ortner, 2003, Schmid et al., 2004), representing the uppermost tectonic unit of the Eastern Alps. Prior to deformation the NCA formed a part of the south-eastern passive continental margin of the Penninic Ocean. Nappe stacking took place mainly in the Cretaceous until Turonian. In contrast the Central Austroalpine, which has been metamorphosed to various degrees up to eclogite facies, the NCA show almost no Alpine metamorphism. In the NCA, Mesozoic carbonates predominate, but also clastic sediments are frequent at several

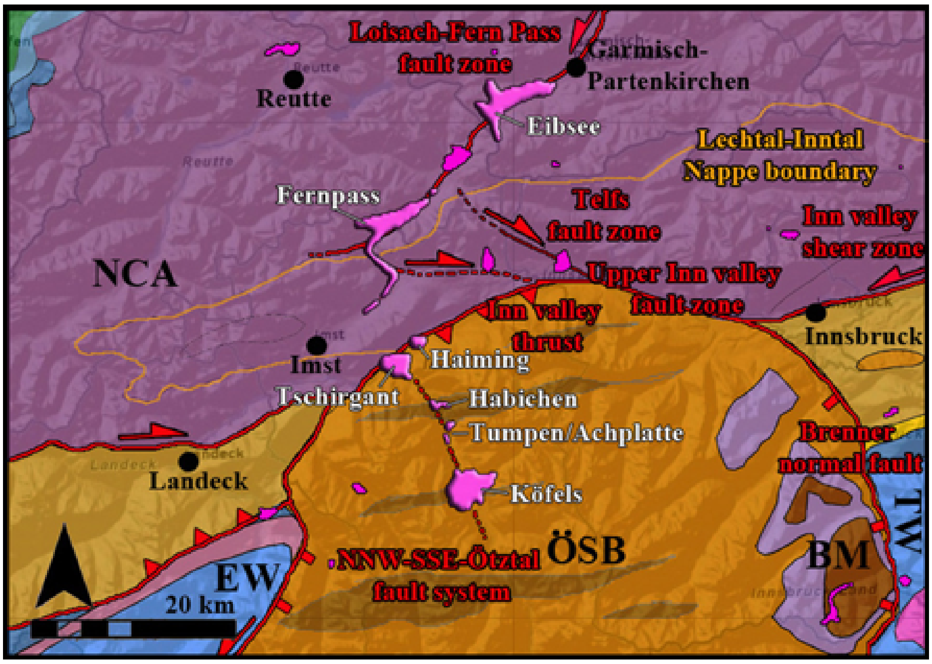

Fig. 2: Geological overview map of the excursion area in western Tyrol, Austria. Deposits of major rock slope failures are indicated in pink colour, labelled ones are in the focus of the excursion. NCA…Northern Calcareous Alps; ÖSB…Ötztal-Stubai Basement; BM…Brenner Mesozoic; TW…Tauern Window; EW…Engadin Window. Major tectonic fault zones are indicated schematically.

stratigraphic levels. The litho-stratigraphic succession sets on in the Permian and locally extends to the Eocene, with thick Triassic rock units being the most prevailing ones. In the excursion area, the NCA can be subdivided into the Inntal nappe (part of the Tyrolic nappe complex) and the Lechtal nappe (part of the Bajuvaric nappe complex).

The **Ötztal-Stubai-Basement (ÖSB)** consists of polymetamorphic rocks with various protoliths of plutonic, volcanic and/or sedimentary origin such as orthogneisses, amphibolites, and thick paragneiss series (mainly biotite-plagioclase-gneisses, metapelites and metapsammites) along with some eclogites and marbles (Hammer, 1929, Purtscheller, 1978). Paragneisses and micaschists prevail and are intercalated with orthogneisses but also amphibolites, eclogites and marbles. The ÖSB was affected by at least six deformation phases (ductile and brittle), with the northern and central areas being characterized by large-scale, gently E-W-striking open folds (Hoinkes & Thöni, 1993, Egglseder & Fügenschuh, 2013).
Concerning the rapid rock slope failures of the ÖSB, predominantly the rigid orthogneisses units were affected, whereas the surrounding incompetent paragneiss series show generally slow slope deformation behaviours. Layering and main foliation of all crystalline rock units are generally E-W-trending and thus orientated unfavourably to promote slope failures. Here the rock mass strength and slope deformation behaviour are controlled by the orientation and geomechanical characteristics of different brittle fracture sets (e.g. Prager et al., 2009b, Zangerl et al., 2010).

Adjacent northwest of the ÖSB, within the NCA, the north-westward thrust of the basement block was accompanied by dextral faulting (**Telfs fault zone,** Fig. 2) with a suggested lateral displacement of 10-15 km (Linzer et al., 2002). Further west, the thrust of the ÖSB and back-thrusting within the NCA have been accommodated by the **Loisach-Fernpass fault zone** (Fig. 2) with an assumed sinistral displacement of 10-15 km (Linzer et al., 2002).
In a regional tectonic context the northern end of the **Brenner normal fault** is kinematically linked with the sinistral **Inn valley shear zone**. Since the early Oligocene, this shear zone accommodated a lateral displacement estimated at 40-50 km (Linzer et al., 2002, Ortner et al., 2006).

It is to be mentioned that the major faults of the Inn valley and Brenner system, as well as the environs of the Telfs and Loisach-Ferpass systems are among the seismically most active zones in the Eastern Alps (Lenhardt et al., 2007, Nasir et al., 2013).
During the Quarternary, the valleys along the excursion route were glacially, fluvio-glacially and fluvially shaped, deepened and filled with various Pleistocene and Holocene sediments to different extents (e.g. Senarclens-Grancy, 1958, Poscher, 1993).

Stop 1: Eibsee rock avalanche

The Eibsee rockslide detached from the north-face of the Zugspitze massif (2962 m), which is the highest summit in Germany. The scarp area is characterized by thick-bedded, and, locally, karstified platform limestones of the Wetterstein Fm. (Ladinian to Carnian). Major fracture systems are to be attributed to the NE-trending Loisach system (Fig. 2).
The volume of rock debris accumulations at Eibsee rock avalanche comprise approximately 400 Mm^3. The area covered with rock debris is about 15 km^2. The run-out distance of about 9.5 km and maximum vertical drop of 2300 m (H/L-ratio: 0.24) yield a runout travel angle (fahrböschungswinkel) of 13.6°. The age of the catastrophic rock slope failure is about 4.1-4.2 ka cal BP based on radiocarbon dated wood fragments from scientific drillings (Jerz & Poschinger, 1995). For further readings reference is made to Golas (1996), Knapp et al., (2015) and Leith et al., (2016) and data sources cited therein.

Some special features of the Eibsee area comprise:

- The prominent lake Eibsee (approx. 1.8 km^2, max. 34.5 m deep) encountered in a morphological depression featuring carbonate

Fig. 3: Panoramic photo of the Eibsee rock avalanche scarp and accumulation area. View in the middle of the image is towards West. The scarp area is situated just below the summit of Zugspitze (2962 m a.s.l.).

bedrocks and Eibsee rock avalanche deposits (Fig. 3); the existence of a paleo-lake prior to the rock avalanche is up for discussion.

- An impressive hummocky landscape, especially east of Grainau, with numerous hills and ridges; here some classical Toma hills are encountered (Fig. 4), i.e. isolated cone- to pyramidal- or roof-shaped hills composed of landslide debris (Abele, 1974, Prager et al., 2006); possible formation processes of these landscape features will be addressed (see also below: Fernpass rock avalanche).
- Preliminary results of ongoing research (drillings, near surface geophysics) carried out by a group from TUM will be presented (Knapp et al., 2015).

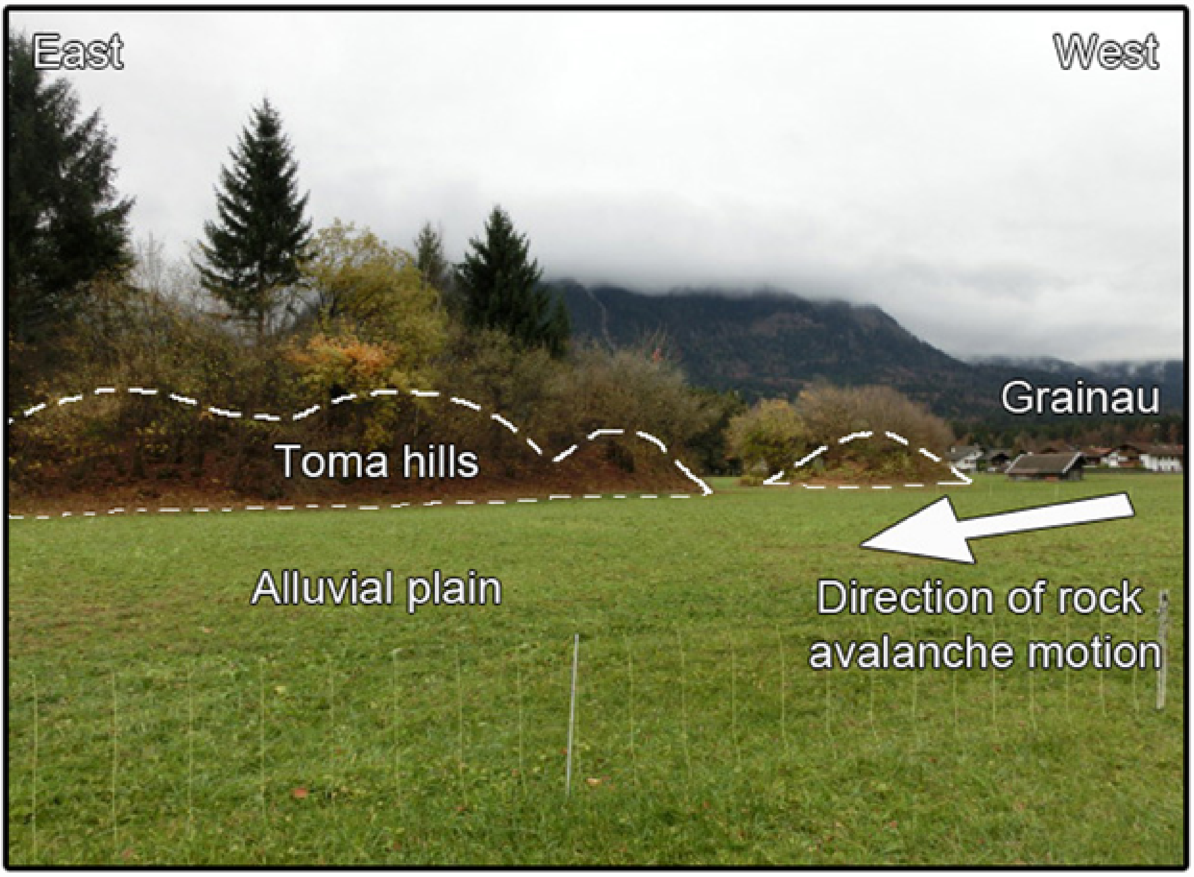

Fig. 4: Typical rockslide morphology of the distal Eibsee rock avalanche deposits featuring cone-shaped Toma hills (east of Grainau, 32T N 652934, E 5260467).

Stop 2: Fernpass rock avalanche

The prominent Fernpass rock avalanche ranges among the largest landslide deposits in the Alps, with a variety of outstanding geological and morphological features (see e.g. Abele 1964, 1974, Prager 2010, Prager et al., 2006, 2009a, 2012). The accumulated landslide debris comprises a volume of approx. 1000 Mm^3, and covers an area of approx. 16.5 km^2 (Fig. 5).
The failing rocks detached from a deeply incised niche made up of several hundred metres thick alternations of platy dolomites, limestones and marls belonging to the bituminous Seefeld Fm., which represent an intra-platform-basin succession within the upper Hauptdolomit Group (Norian). The unusually shaped scarp indicates that this wedge failure was not only due to the existing rheology and bedding conditions, but above all due to complex intersections of uncemented fault systems and fracture zones (Prager, 2010). As a striking feature, the slide debris devided into two separate arms: i) the northern rockslide branch, which contains the majority of the failing debris and extends at least 11 km onto the aggradation plain of the Lermooser Moos and ii) the southern branch, which contains a smaller volume and has larger deflection angles, but nevertheless shows an amazingly greater runout of up to 15.5 km (Fig. 5) (Prager et al., 2006, 2009a, 2012). The maximum vertical drop of 1270 m for the northern branch results in a fahrböschungswinkel of 6.7°, the southern branch shows a maximum vertical drop of 1440 m and results in a fahrböschungswinkel of 5.3° (H/L-ratio north: 0.12; H/L-ratio south: 0.09).
The age of the rock slope collapse at Fernpass was determined by applying three independent radiometric dating methods to geologically individual sample sites. The dating data comprise i) Cl-36 surface exposure ages determined for exposed sliding planes at the scarp and for boulders within the accumulation area, ii) C-14 data of rockslide-dammed torrent backwater deposits, iii) U/Th-dating of post-depositional aragonite cements encountered beneath and between accumulated boulders (Ostermann et al., 2007, Prager et al., 2009a, Prager, 2010). The obtained data coincide well and indicate a rapid failure and accumulation event at about 4.2 ka.

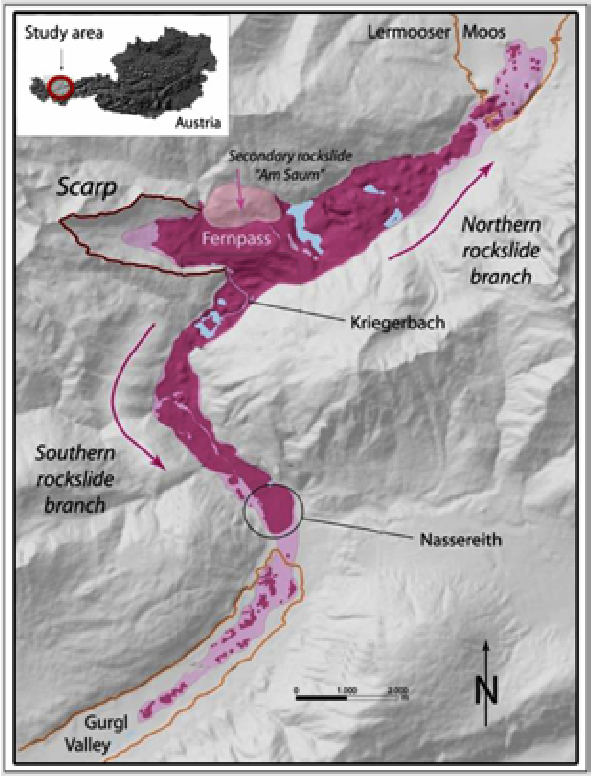

Fig. 5: LiDAR derived hillshade model of the Fernpass area showing the scarp and the accumulation area of the rock avalanche deposits (dark pink: field outcrops of rock avalanche deposits; light pink: assumed accumulation area; light blue: lakes ontop of the rock avalanche deposits; orange line: top of lacustrine deposits, underlying the rock avalanche debris) (Prager et al., 2006).

Some special features of the Fernpass area comprise:

- Complex travel path of the Fernpass rock avalanche: due to the oblique impact on its opposite slope (Fig. 5, Fig. 6 & Fig. 7), the failing rock masses were proximally piled up to a thick succession and subsequently split into two channeled but diametrically opposed rock avalanche branches; geophysical investigations (hybride seismics around the present-day Fernpass) indicate a parabolic bedrock valley cross-section and a thicknesses of the overlying material of some 100 m.
- Extremely long run-out of the rock avalanche branches: empirical correlations of volumes and runout distances will be debated as well as results obtained from drilling campaigns and geophysical investigations (seismics, -GPR); since evidence is given that at least the medial to distal Fernpass landslide debris

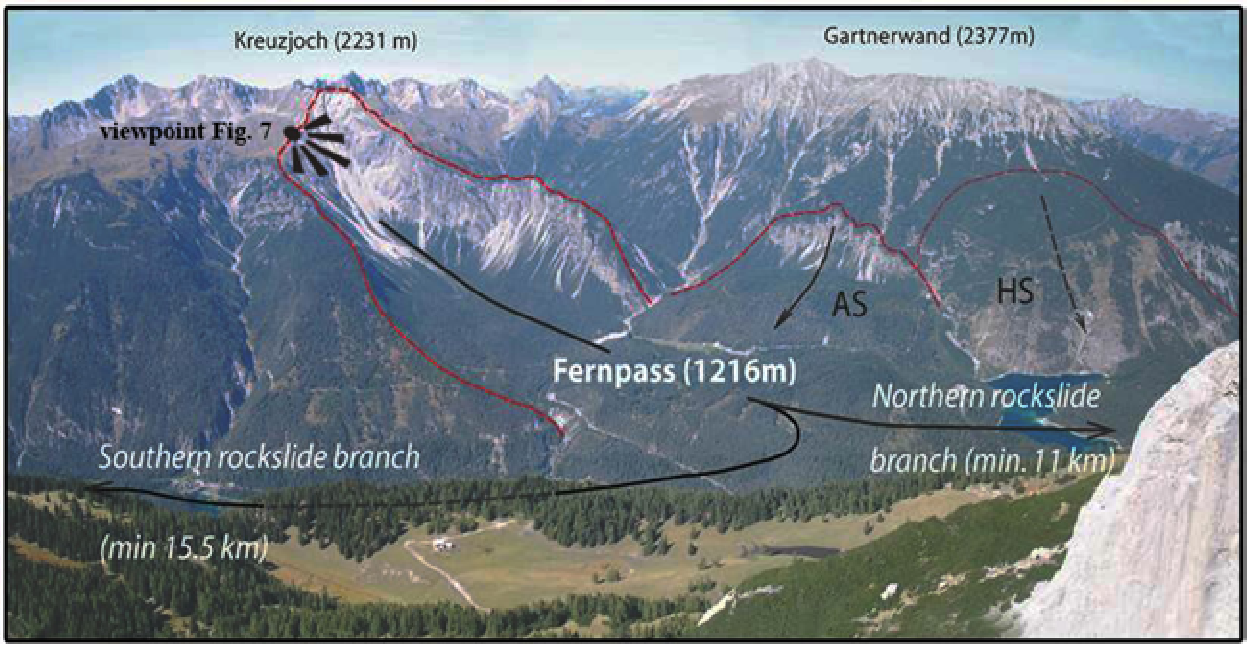

Fig. 6: View towards NW to the wedge-shaped scarp of the Fernpass rock avalanche and adjacent landslides (rockslide "Am Saum" AS, fractured slope "Hohler Stein" HS, from Prager et al., 2008).

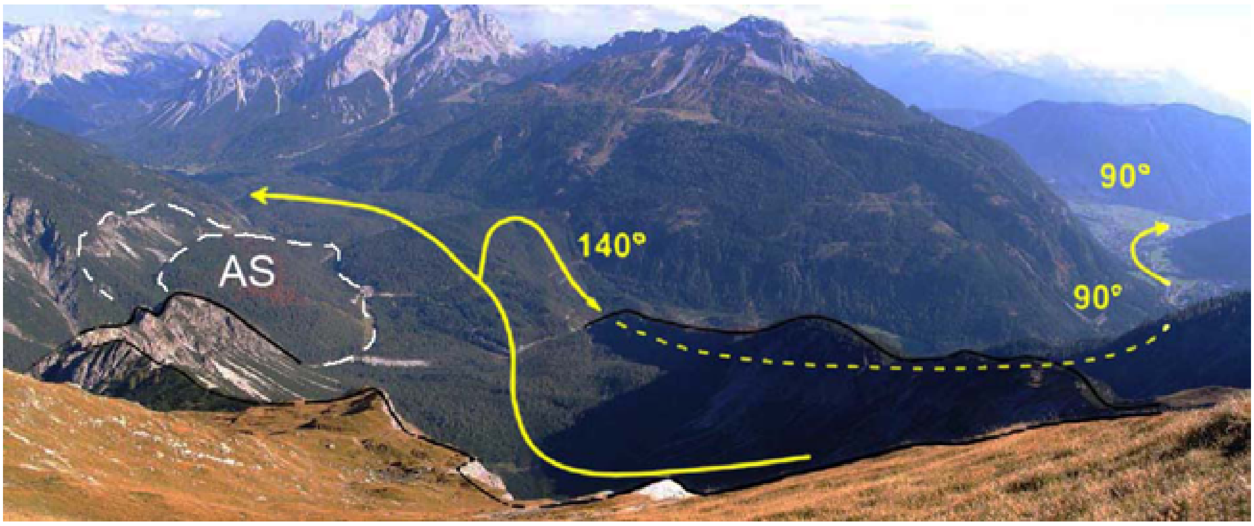

Fig. 7: Down view from the Fernpass scarp towards NE to the proximal accumulation area. The yellow lines indicates the rock avalanche run-out path whereas the numbers show the change in direction in angular degrees. Note thick pass wall and split into two opposed branches. Secondary rockslide "Am Saum" (AS) is schematically indicated.

surged upon low permeable, saturated soils, hydro-mechanically landslide processes will be addressed; major graben structures (some filled with kettle-like lakes) and striking Toma hills around Biberwier and Nassereith; possible formation processes of these landscaping features will be debated (see also above: Eibsee rock avalanche).

- Striking hydrogeological features (significant springs, tested flow/discharge rates, radon emanations, etc.).

Stop 3: Tschirgant Rock Avalanche

From the steep and rugged Tschirgant massif (2370 m), two deep-seated rockslides travelled down to the river Inn at approximately 700 m a.s.l.: the prominent Tschirgant rockslide in the southwest and the smaller Haiming rockslide in the northeast (Fig. 8; see also Stop 4). Both slope failures are encountered at the structurally complex southern margin of the Inntal thrust sheet (Northern Calcareous Alps) (Fig. 2), which in this area is made up of folded and faulted Middle- to Upper-Triassic carbonates (Eisbacher & Brandner, 1995, GBA, 2011, Prager et al., 2016).

The lithological and structural conditions encountered show that the failure of the competent dolostones and limestones of the Wetterstein-Fm. (M-Triassic) is to be attributed to intensely faulted fold structures (Pagliarini 2008). The geological setting suggests that this slope collapse was mechanically favoured by the presence of weak Raibl beds at the toe of the slope. Locally, intensely mineralised springs in this area are furthermore a sign of hydrochemical evaporite leaching of the Raibl rauhwacke strata und thus of a correspondingly reduced slope stability (Prager, 2010, Prager et al., 2008, 2012).

The volume of rock debris accumulations at the Tschirgant rock avalanche is approximately 200-250 Mm^3, the area covered with rock debris is about 10km^2 (Patzelt, 2012, Dufresne et al., 2016a, Ostermann et al., 2016) (Fig. 9). A run-out distance of about 6.2 km and a maximum vertical drop of 1400 m (H/L-ratio: 0.23) results in a run-out travel angle (Fahrböschungswinkel) of 12.7°.

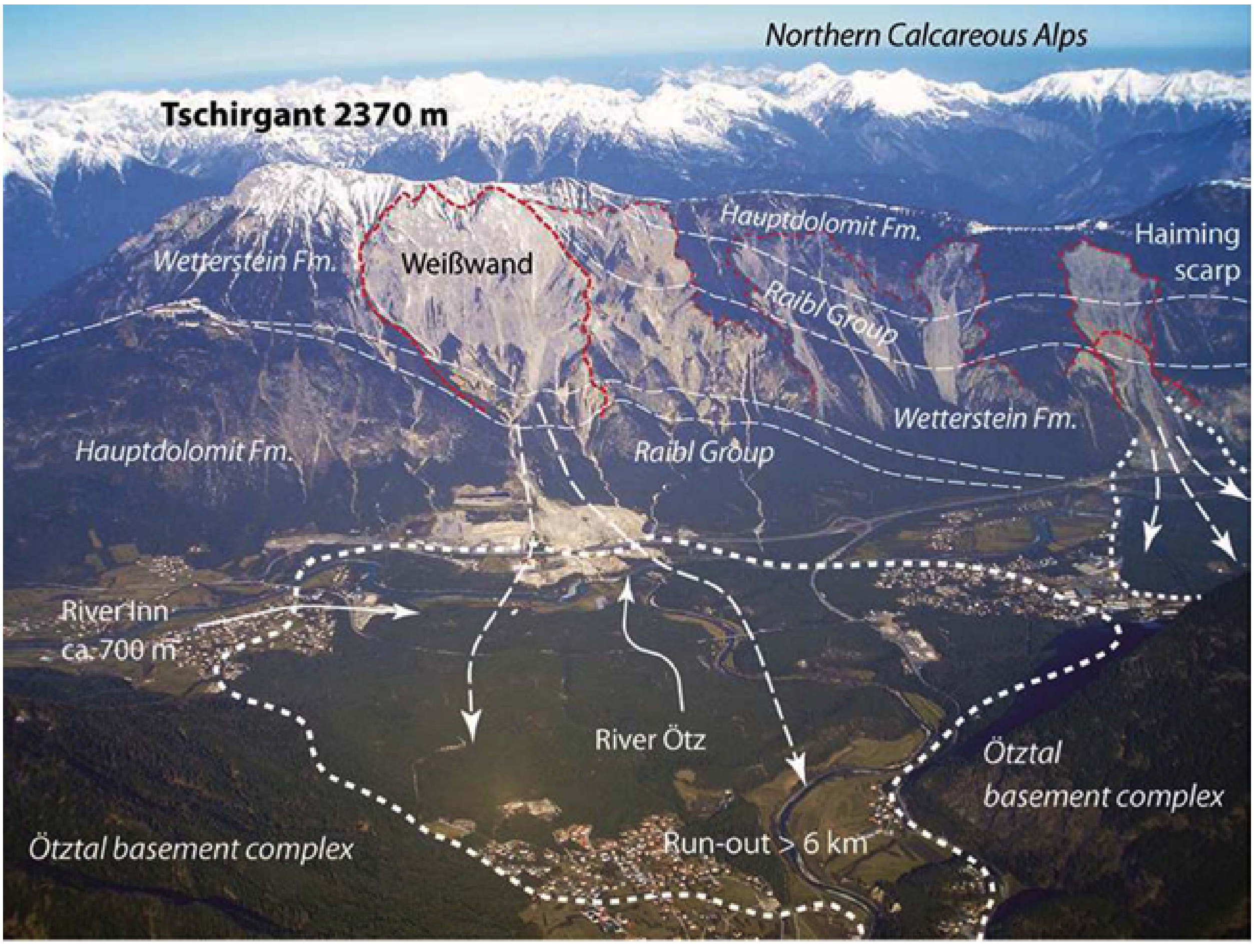

Fig. 8: Oblique view from the northern Ötz valley to the Inn-valley and Tschirgant massif. Scarp (red stippled) and accumulation areas (white stippled) of the Tschirgant and Haiming rock avalanches. The major tectono-stratigraphic units are indicated schematically, complex fold and fault structures here not depicted (from Prager et al., 2008).

Based on several radiocarbon datings, the Tschirgant event dates into the M-Holocene (Patzelt & Poscher, 1993), with two inferred events occurring at about 3650-3450 and 3150-2950 yrs cal BP respectively (Patzelt, 2012). However U/Th-dating and surface exposure dating combined with all available radiocarbon dates indicate only one accumulation event at 3014±62 yrs BP (Ostermann et al., 2016). These ages are somewhat younger than those obtained for the rock avalanches at Eibsee, Fernpass, Haiming and Stöttlbach (see Prager et al., 2008).

In the Toma landscape, which is comparable to the Fernpass area, geometrically partially complex sedimentary structures are encountered, featuring carbonate rockslide debris associated with polymict fluvial sediments (Patzelt & Poscher, 1993, Abele, 1997). Drilling data (TIRIS 2016) and natural outcrops show that the Tschirgant rockslide not only overlies fluviatile sands and gravels, but is partially dynamically mingled with and even overlain by the same. The latter and maybe also the allochthonous plants found atop the carbonate rockslide deposits, indicate that both

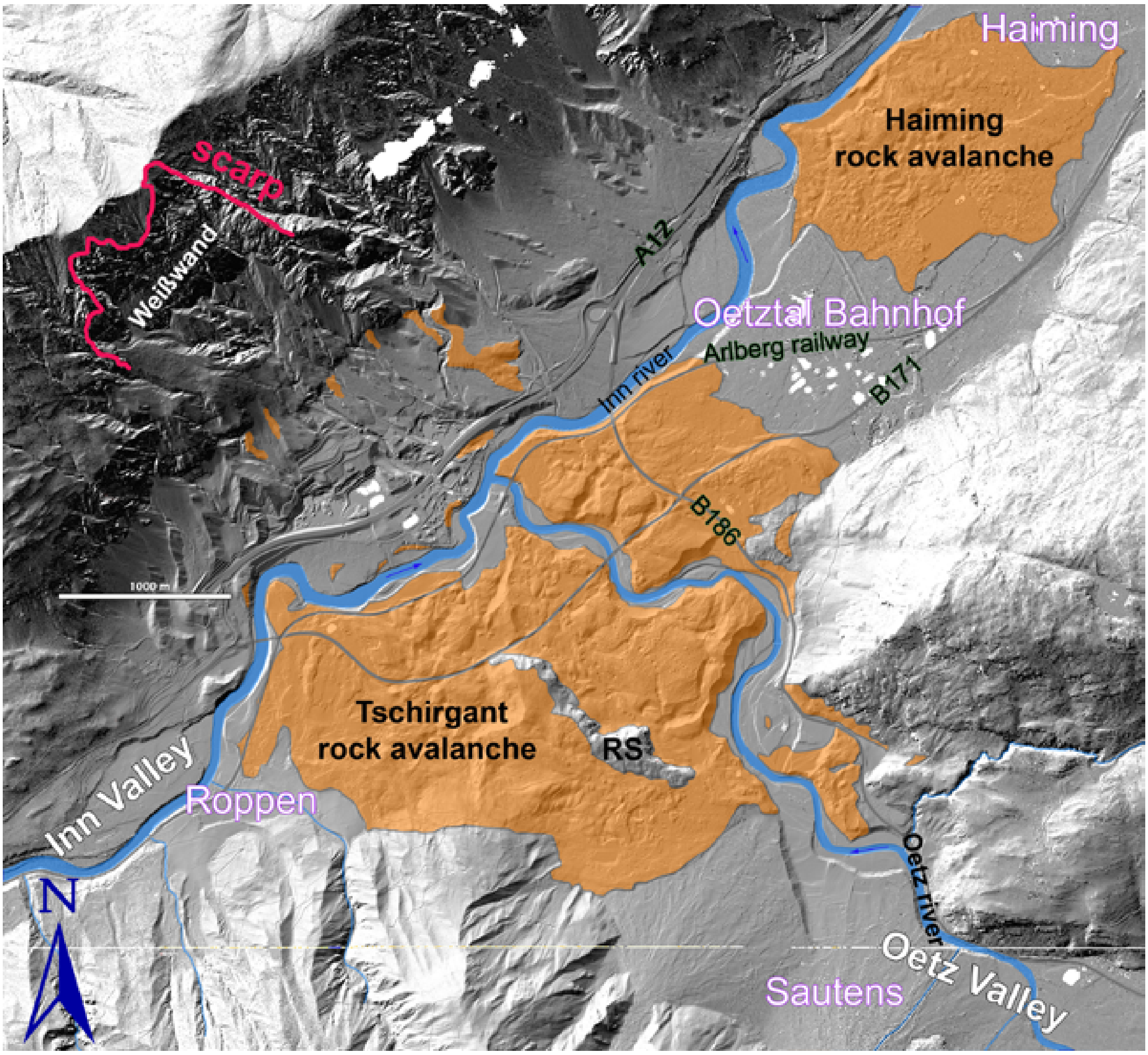

Fig. 9: Airborne laserscan image (TIRIS) with outlined deposits of the Tschirgant rock avalanche. Note fluvial incision of the rivers Inn and Ötz, providing some well-exposed outcrops. RS…"Rammelstein" bedrock outcrop of Ötztal-Stubai basement rocks.

were transported piggy-back from the scarp area on top of the slide/fall masses and that kinematically the "Bergsturz" event was characterised by laminar flow processes (Prager, 2010, Prager et al., 2012, Dufresne et al., 2016a).

Special features:

- Geological field mapping and the thus obtained lithological distribution shows that the Tschirgant deposit retained source stratigraphy to a large extent (Dufresne et al., 2016a). This preserved slope stratigraphy argues against chaotic rock avalanche movements but further indicates laminar slide/flow movements of the rockslide.
- Geological subsurface information on the Tschirgant deposit (e.g. thickness and grain size distributions) and its substrate can be obtained from geological borehole logs (TIRIS 2016).
- One outstanding feature of the Tschirgant rock avalanche is that the contact of the basal slide deposits with the valley substrate is locally well exposed. The contact zone displays complex geometries, where in the course of the rockslide event presumably water-saturated valley floor sediments were injected into the rockslide masses filling up steep extension structures and where diamicts were created by mingling with the rock avalanche (Patzelt & Poscher,1993, Abele, 1997, Prager, 2010, Prager et al., 2012, Dufresne et al., 2016a).
- Locally, precipitation of post-depositional carbonate cements, enabling U/Th-age dating of the event (Sanders et al., 2010, Ostermann et al., 2016).
- Large post-failure debris flows lapping onto the proximal rock avalanche deposits (e.g. location Breitmure, see also Stop 4).

Stop 4: Haiming Rock Avalanche

About three kilometres northeast of the Tschirgant scarp (see Stop 3), the Inn valley floor is covered by the carbonate Haiming rock avalanche deposits (Fig. 9). The source area is made up of steeply SE-dipping carbonates of the Wetterstein Fm. (GBA, 2011, Prager et al., 2016). The accumulated debris, i.e. karstified dolostones, breccias and limestones of the topmost Wetterstein Fm., indicates that the rock avalanche detached from lower parts of the slope; the exposure of higher regions of the present-day scarp, which show a several hundred metre thick, well-bedded succession of the lithologically inhomogeneous Raibl Group and the Hauptdolomit Fm (both U-Triassic), may be attributed to secondary erosion processes such as rockfalls and debris slides (Prager et al., 2008) (Fig. 10). The volume of rock debris accumulations at the Haiming rock avalanche was estimated to range approximately between 25-34 (Abele, 1974) and 50-60 (Patzelt, 2012) Mm^3, but new calculations indicate a much smaller volume of 10-15 Mm^3 (Dufrese et al, 2016b). The area covered with rock debris is about 2.3 km^2. A run-out distance of about 2.4 km and a maximum vertical drop of 550 m (H/L-ratio: 0.20) results in a run-out travel angle of 12.9°. Locally, in construction pits the basal carbonate debris and its substrate i.e. fluvial sediments were exposed (Patzelt, 2012).
Based on radiocarbon datings, the age of the Haiming rock avalanche is 3500-3000 yrs cal BP, with a minor event occurring at 1820-1540 yrs cal BP (Patzelt, 2012). Based on field surveys two failure events are not indicated yet.

Special features:

- Geological setting at the scarp area well-known due to geological borelogs obtained from a subhorizontal drilling into the lower scarp slope (TIRIS 2016).
- Accumulated debris containing some reddish (paleo-karstified) often finely ground carbonates, with rather few mega-blocks encountered atop.
- LiDAR images reveal that fluvial terraces are encountered underneath the thin cover of rock avalanche debris. Tracing back such a pre-Haiming rock avalanche terrace upstream along the Inn River, we find that this terrace cuts through the Tschirgant deposits. Therefore, the rock avalanche at Haiming must be younger than those at Tschirgant, irrespectively of radiometric dating results.
- Post-failure debris flows lapping onto the proximal rock avalanche deposits (location Galgenmure; Sanders, 2012).

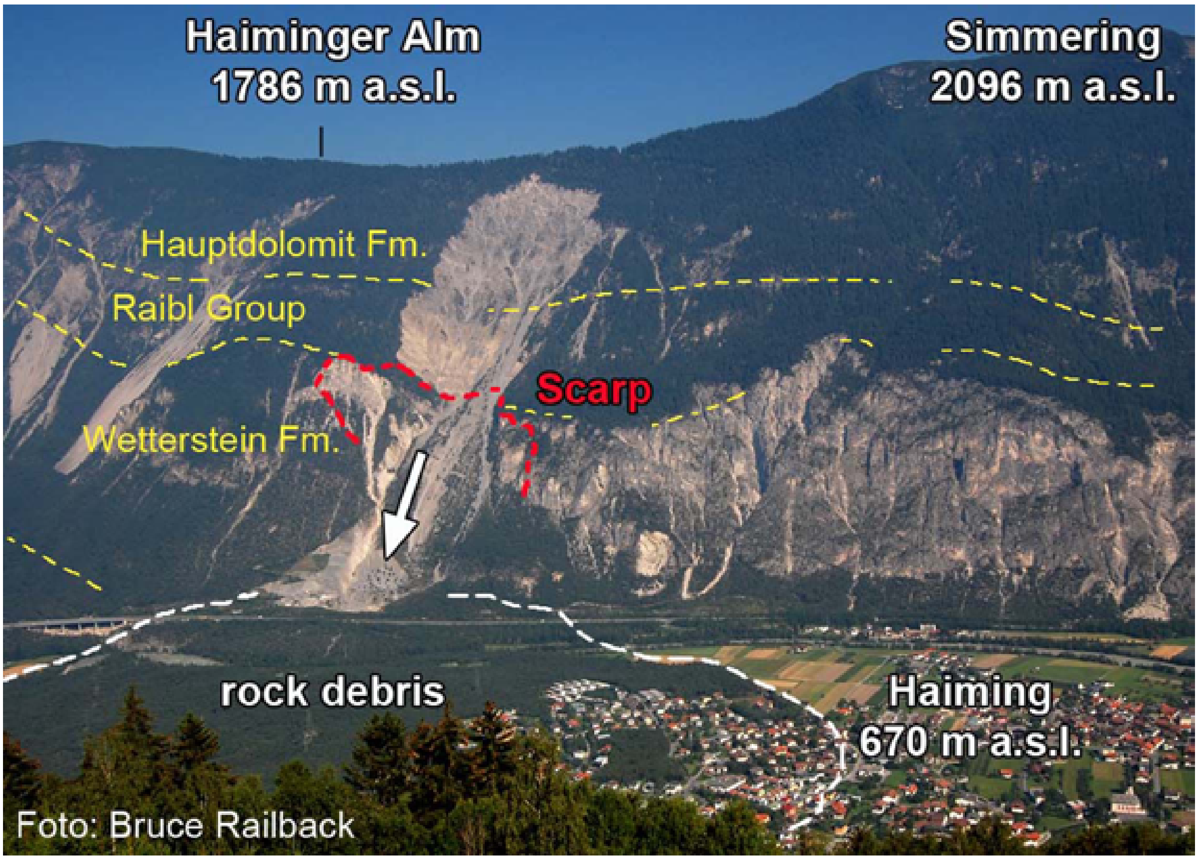

Fig. 10: Oblique view to the south-east facing Tschirgant-Simmering ridge, with scarp of the Haiming rock avalanche (red dashed line) and main lithological units schematically indicated. The carbonate debris (Wetterstein Fm.) spread out over the alluvial valley bottom.

Stop 5: Habichen Rock Avalanche

At the entrance of the Ötz valley the first crystalline rock debris accumulations at the valley floor belong to the Habichen rock slope failure (Fig. 11)

The scarp area of the Habichen rock avalanche is characterised by massive granodiorite gneisses (Hammer, 1929, GBA, 2011, Rothmund, 2012, Ostermann & Prager, 2014). The volume of rock debris accumulations at the Habichen rock avalanche is approximately 27 Mm^3. The area covered with rock debris is about 1.2 km^2. A runout distance of about 2.9 km and a maximum vertical drop of 950 m (H/L-ratio: 0.32) results in a run-out travel angle of 18.2°.

^{14}C analyses of lacustrine deposits, obtained from drillings in the central part of the lake, yielded an age of 11500 cal yrs BP (Wahlmüller, unpubl. data) and indicate a minimum age for the Piburg rockslide barrier (Prager et al., 2008).

Special features:

- The Habichen rockslide dammed two surface discharge systems: one at Lake Piburg (Fig. 11 & Fig. 12) which has been dammed in the south by the rock avalanche dam, and another at Habichen, i.e. backwater sediments of the river Ötz, where the rockslide dam failed and an outburst flood occurred (indicated by field morphology and LiDAR hillshade images).

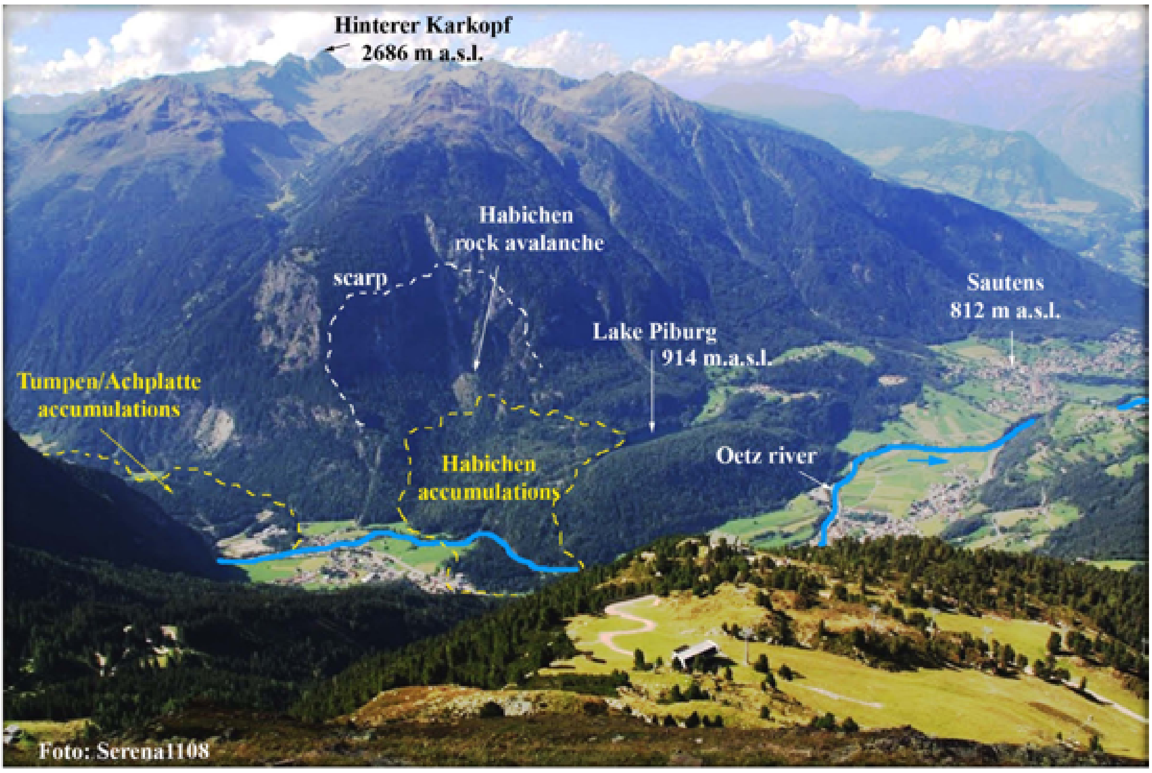

Fig. 11: Norther Ötz valley, oblique view towards West. The Habichen rock avalanche left a well-developed niche and dammed the still existing Lake Piburg as well as the river Ötz in the main valley.

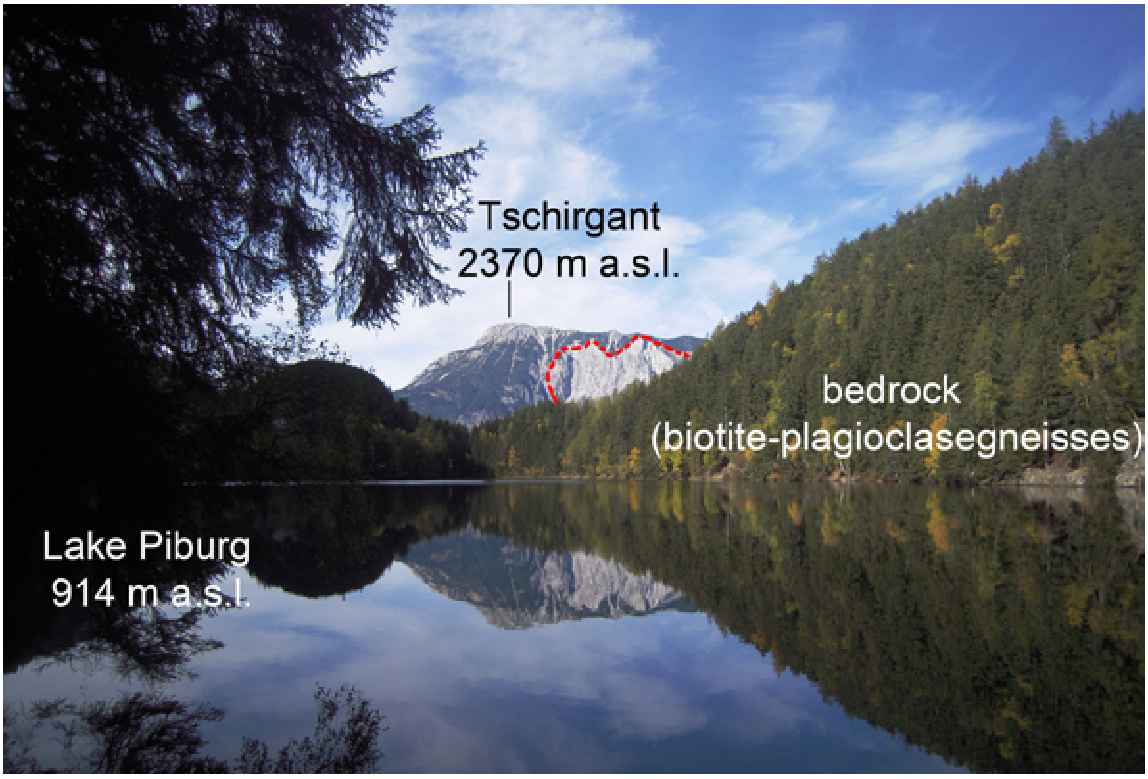

Fig. 12: View from the banks of Lake Piburg towards North-West. The Habichen rock avalanche dammed a pre-existing bedrock depression of glacial origin at its southern margin and thus dammed Lake Piburg. In the background upper part of the scarp area of the Tschirgant rock avalanche (Stop 3).

Stop 6: Tumpen/Achplatte Rock Avalanche

The Tumpen area is characterised by a significant valley step and a flat upstream valley floor (Fig. 13), which genetically may be attributed to several individual landslide events and associated backwater sediments (Heuberger 1975, Poscher & Patzelt, 2000).

The major Tumpen/Achplatte rock avalanche detached from a granodiorite gneiss unit (Hammer, 1929, GBA, 2011) at the eastern valley flank of the Ötz valley (Fig. 13 & Fig. 14). The accumulated debris comprises a volume of approximately 60 Mm^3, and covers an area of about 0.6 km^2. A runout distance of about 2.2 km and a maximum vertical drop of 900 m (H/L-ratio: 0.41) results in a run-out travel angle of 22.3°.

The age of the Tumpen/Achplatte rock avalanche is not known to date. However, radiocarbon dates of fluvio-lacustrine backwater sequences provided an age of about 3840-3440 yrs cal BP (Poscher & Patzelt, 2000), which is a minimum age for the damming event (most likely Achplatte rock avalanche).

Special features:

- At the location "Eiskeller", thermally-induced chimney effects (comparable with dynamic ice-caves) reduce the temperature of the air circulating within the pore space of the lower parts of blocky rockslide debris to below the outside air temperature (Fig. 14) .
- Within the backwater basin of the Tumpen/Achplatte rock avalanche, now filled by fluvio-lacustrine sediments, sinkhole collapses in valley floor sediments have been documented repeatedly over the last 300 years. This led to geological subsurface investigations and mapping of the deposits of different rock slope failures (Poscher & Patzelt, 2000).

Fig. 13: Oblique view of the Oetz valley at Tumpen towards North. The valley was dammed by the Tumpen/Achplatte rock avalanche and the Tumpen backwater basin filled up with fluvio-lacustrine sediments. Other landslide events in the area Tumpen village (Poscher & Patzelt, 2000) here only indicated schematically (orange lines). The river Ötz incised into the rock avalanche debris (granodiorite gneiss) and now cascades down over a vertical distance of 90 m within just about 500 m in horizontal distance, known as the "Achstürze".

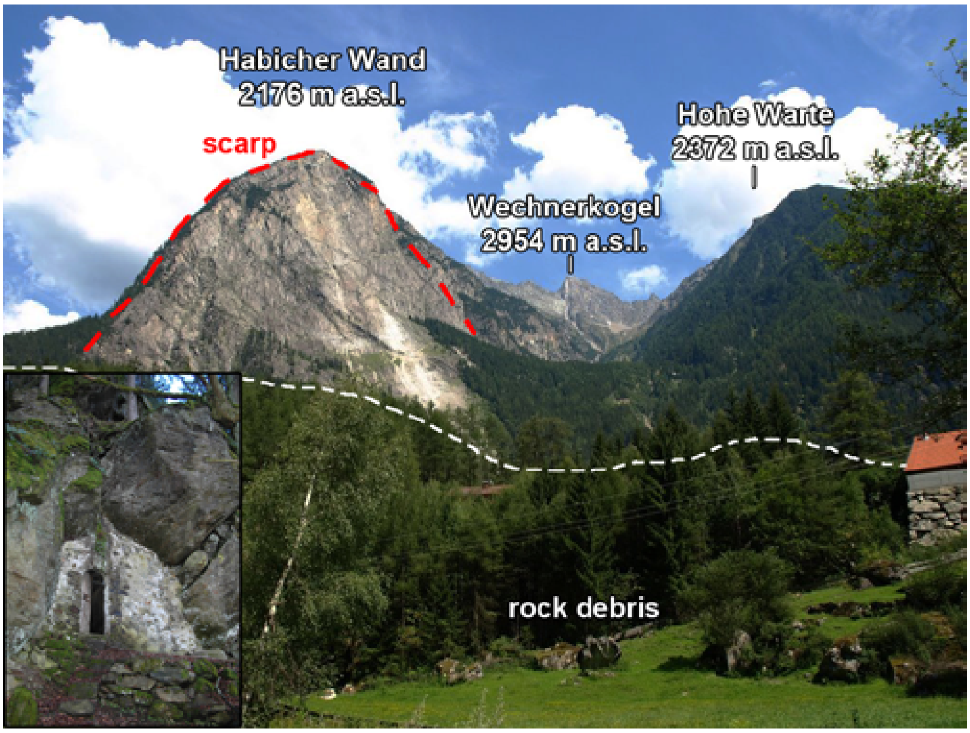

Fig. 14: Scarp area of the Tumpen/Achplatte rock avalanche. View towards ENE. The main scarp area is represented by the Habicher Wand (red line). The insert foto shows the "Eiskeller" at the most distal sections the Tumpen/Achplatte rock avalanche. To increase the local cooling effects (see text below), damming stone walls were built in the 17th century.

Stop 7 & Stop 8: Köfels rockslide

The prominent Köfels rockslide is the largest crystalline mass movement in the Alps (Abele, 1974). Due to the enormous volume and the occurrence of "pumice" (Pichler 1863), these rockslide deposits have been subject to scientific research for about 150 years. Its slide debris detached from an east-facing slope and left a giant niche, where the geological and structural conditions are well exposed (Fig. 15, Fig. 16 & Fig. 17). According to the lithologies encountered in the scarp and accumulation area, the main source of the rapid Köfels rockslide is represented by a several hundred metres thick orthogneiss complex embedded in thick paragneiss series (Hammer,1929, GBA, 2011). Field surveys show that both layering and foliation are orientated unfavourable to promote slope failures, but that this slope collapse was clearly structurally predisposed the coalescence of different brittle fracture systems (Prager et al., 2009b).

The volume of rock debris accumulations of the Köfels rockslide is approximately 3900 Mm^3 (Brückl, 2001) (Fig. 16 & Fig. 17). The area covered with rock debris is about 11.5 km^2, with the isolated distal deposits at Lärchenbühel (Tumpen backwater plain, see Stop 4) indicating a somewhat larger spatial distribution. A runout distance of about 6 km and a maximum vertical drop of assumed 1700-1900 m (H/L-ratio: 0.28-0.32) results in run-out travel angle of 15.8° (depending on assumed top paleo-scarp and which distalmost accumulations considered).

The age of the Köfels rockslide was determined based on radiocarbon dating of wood found in an investigation adit (Heuberger 1966), surface

Fig. 15: Overview image of the Köfels rockslide area view towards WNW. The rockslide mass detached along East-dipping sliding planes and fully dammed the Oetz valley. The resulting Längenfeld backwater basin was filled up with decametre-thick fluvio-lacustrine sediments. Now the river Ötz is deeply incised in the rockslide debris, forming the Maurach gorge but not exposing the base of the rockslide yet.

exposure dating (Ivy-Ochs et al., 1998), and recently fixed more precisely with tree-ring analyses, pointing to an event at 9527-9498 cal BP (Nicolussi et al., 2015, and references therein).

Special features:

- An outstanding feature of the famous Köfels site is the occurrence of frictionites ("pumice", "Köfelsit", "hyalomylonites") (Fig. 18). These fused rocks formed due to the friction heat, which developed on shear planes during the rapid sliding movement (Preuss, 1974, Erismann et al., 1977). The frictional melting of the Köfels (ortho-)gneisses along distinct sliding planes resulted from very high strain rates due to the volume (thickness) and velocity of the rockslide mass. Stop 7: Maurach gorge (32 T 646426, E5220728).
- Extremely high radon concentrations attributed to dynamic rock fragmentation are measured in the Umhausen area. The highly crushed orthogneisses of the Köfels rockslide and the thus increased areas of active rock surfaces are the primary source of the radioactive noble gas ^{222}Rn emanations (Purtscheller et al., 1995). Stop 7: Maurach gorge (32 T 647989, E5218302)
- The Köfels rockslide debris fully blocked the Ötz river and caused the accumulation of up to 100 m-thick fluvio-lacustrine backwater deposits within the Längenfeld basin (Klebelsberg, 1951). According to drilling data and reflection seismic surveys, the top of the bedrock units plunges from approximately 50-80 m below ground in the Längenfeld basin steeply northwards to approximately 400 m below ground at the palaeo-slope toe (Brückl et al. 2001). Stop 7: Maurach gorge (32 T 647989, E5218302)
- Rockslide-transported glacial scratch marks and the origin of fluviatile deposits on top of rockslide deposits will be discussed. Stop 8: Niederthai, (32 T 648795, E 5218302)

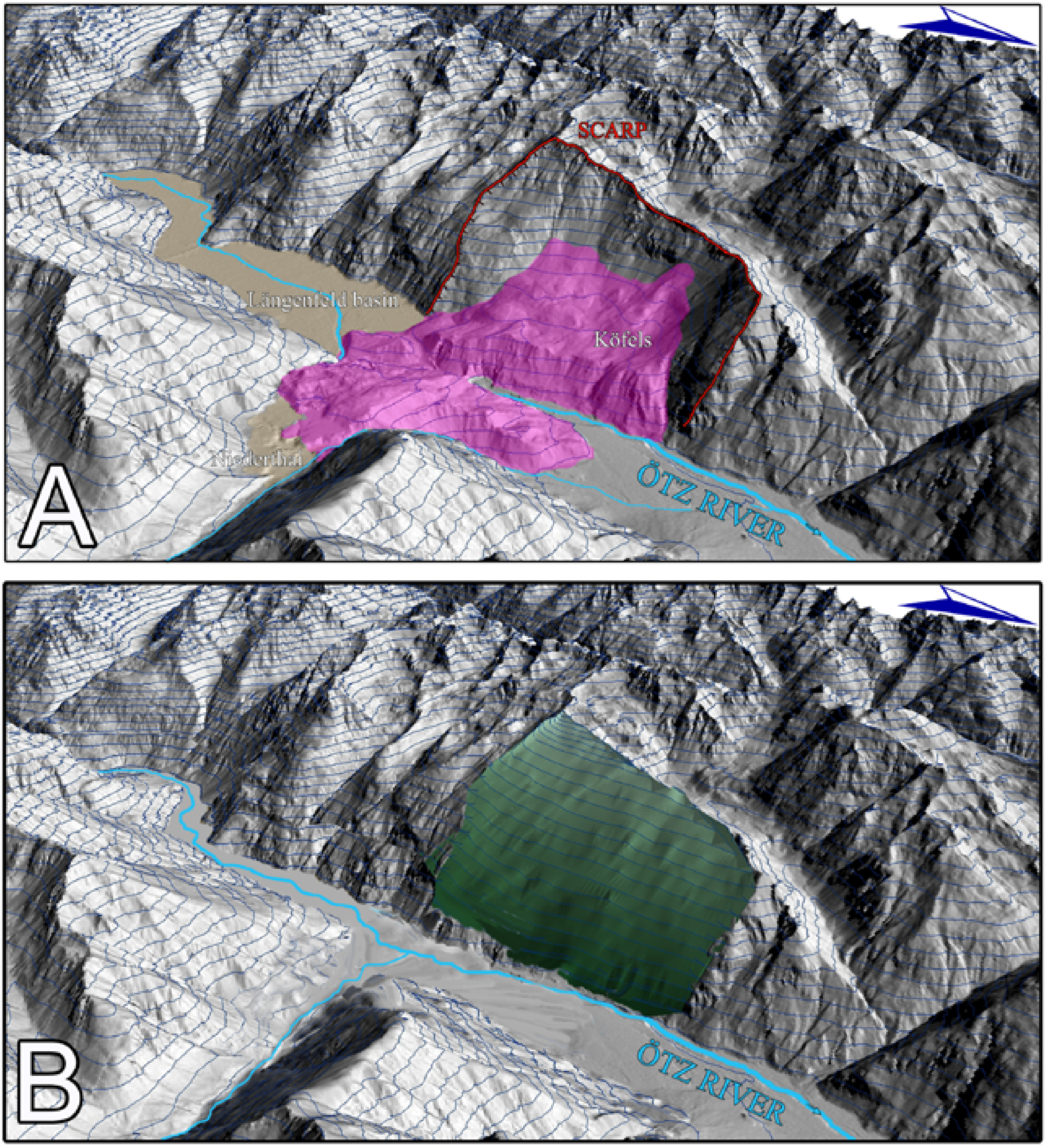

Fig. 16: LiDAR derived hill-shade model of the central Ötz valley. **(A)** Present-day situation, showing that the Köfels rockslide dammed the main valley (Längenfeld basin) as well as the Horlach valley at Niederthai. Now the river Ötz is deeply incised in the rockslide accumulations. **(B)** Reconstructions of the pre-failure situation at Köfels. Higher elevation of the pre-failure ridge considered, geometry of the pre-failure slope toe not considered in detail (for pre-failure cross sections see Brückl et al., 2001, Prager et al., 2009b).

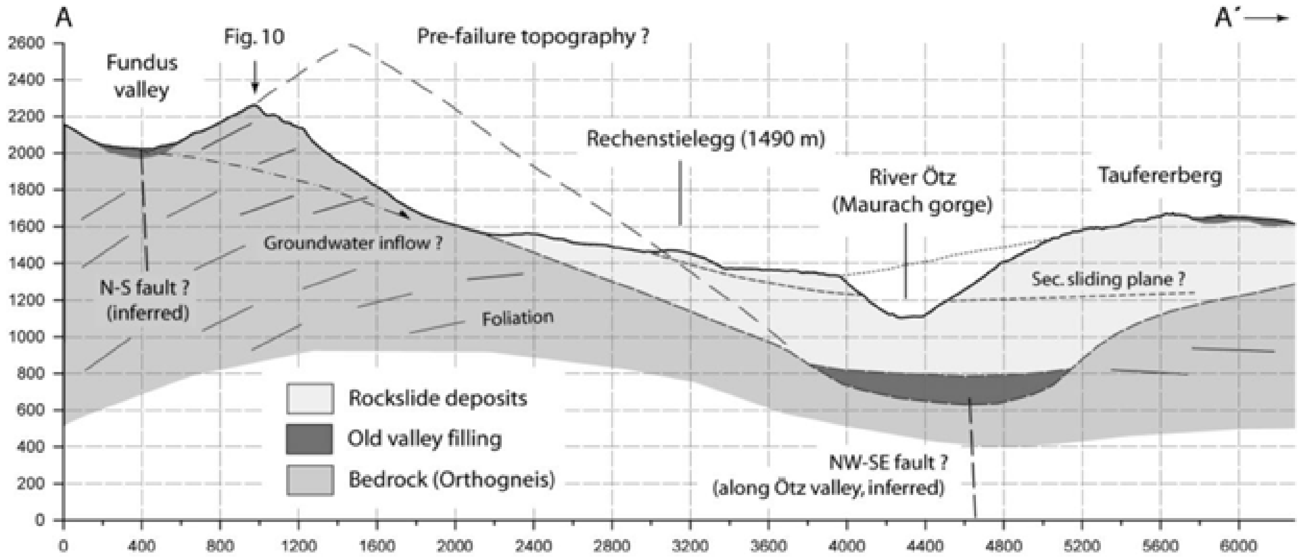

Fig. 17: Geological cross section of the Köfels rockslide (Prager et al., 2009b; thickness of slide debris according to Brückl et al., 2001).

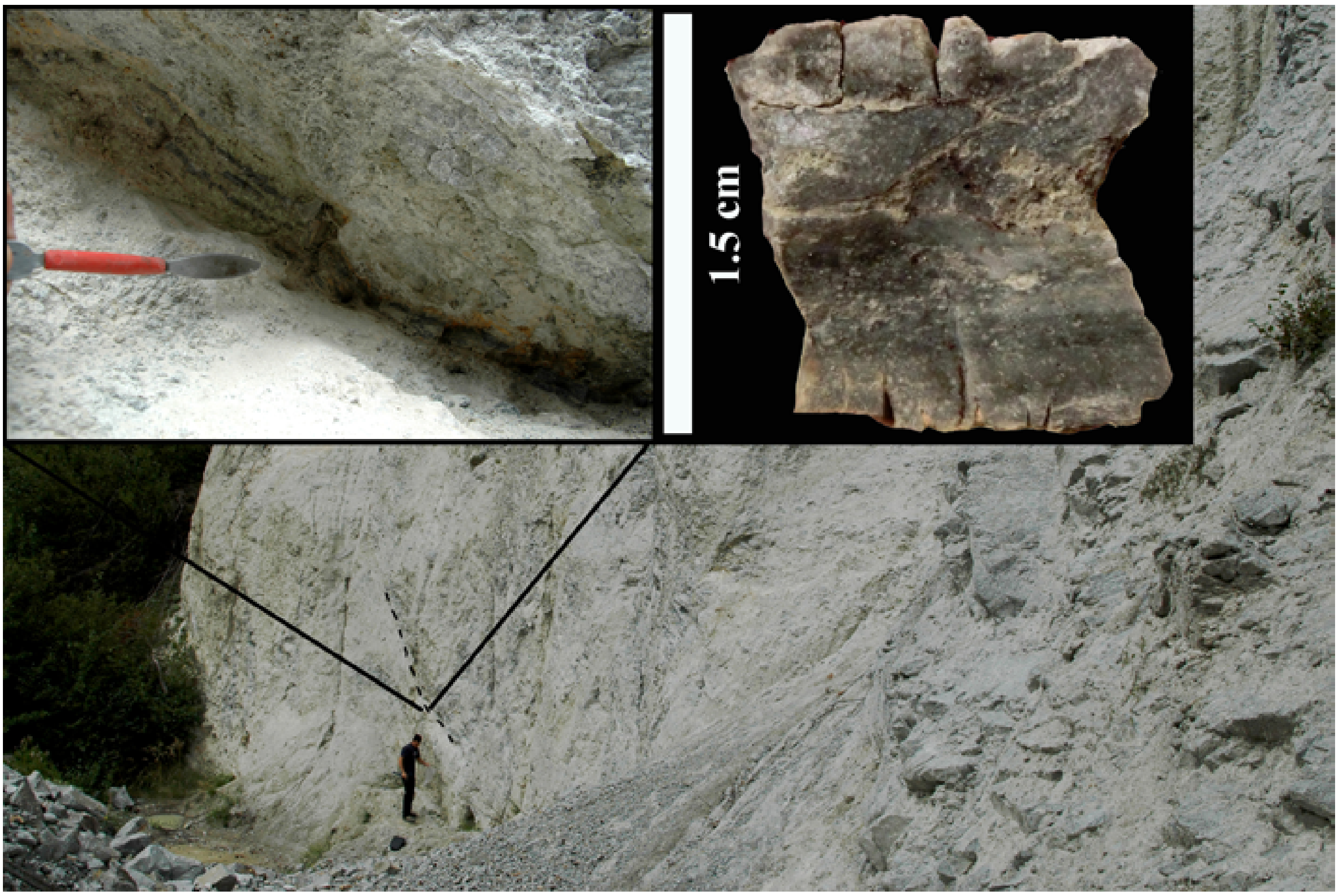

Fig. 18: Outcrop situation of the hyalomylonite (frictionite). Along a distinct shear plane in between intensively crushed orthogneisses a 0.5 to 3 cm thick lens of glassy fused rock is developed. Further above (out of the image) an intensely crushed but only slightly sheared diabase dyke is encountered. Stop 7: Maurach gorge (32 T 646426, E5220728).

References:

Abele, G., 1964: Die Fernpaßtalung und ihre morphologischen Probleme.– Tübinger Geograph. Stud. 12, 1-123.

Abele, G., 1974: Bergstürze in den Alpen, ihre Verbreitung, Morphologie und Folgeerscheinungen. Alpenvereinshefte 25, 1-230.

Abele, G., 1991: Der Fernpassbergsturz. Eine differentielle Felsgleitung. Österr. Geograph. Ges., Zweigver. Innsbruck Jhrber., 1989/1990, 22–32.

Brückl, E., 2001: Cause-Effect Models of Large Landslides. - Natural Hazards 23, 291-314.

Brückl, E., Brückl, J., Heuberger, H., 2001: Present structure and prefailure topography of the giant rockslide of Köfels. Zs. Gletscherkde. Glazialgeol. 37, 49-79.

Dufresne, A., Prager, C., Bösmeier, A., 2016a: Insights into rock avalanche emplacement processes from detailed morpho-lithological studies of the Tschirgant deposit (Tyrol, Austria). Earth Surface Processes and Landforms, 41, 5, 587-602.

Dufresne, A., Ostermann, M., Kelfoun, K., Ring, M., Asam, D., Prager, Ch., 2016b: A revision of the Haiming rock avalanche (Eastern Alps). Geophysical Research Abstracts, 18, EGU2016-7701.

Egglseder, M., Fügenschuh, B., 2013: Pre-Alpine fold interference patterns in the Northeastern Oetztal-Stubai-Complex (Tyrol, Austria). Austrian Journal of Earth Sciences, 106/2, 63-74.

Eisbacher, G.H., Brandner, R., 1995: Role of high-angle faults during heteroaxial contraction, Inntal Thrust Sheet, Northern Calcareous Alps, Western Austria. Geol. Paläont. Mitt. Innsbruck 20, 389-406.

Erismann, T.H., Heuberger, H., Preuss, E., 1977: Der Bimsstein von Köfels (Tirol), ein Bergsturz "Friktionit". Tschermaks Mineralogisch-Petrographische Mitteilungen, 24, 67-119.

GBA, 2009: Geofast 1:50.000, Zusammenstellung ausgewählter Archivunterlagen der Geologischen Bundesanstalt, Blatt 115 – Reutte (Ausgabe 2009/10), Geologische Bundesanstalt, Wien.

GBA, 2011: Geofast 1:50.000, Zusammenstellung ausgewählter Archivunterlagen der Geologischen Bundesanstalt, Blatt 116 – Telfs (Ausgabe 2011/04), 145 – Imst (Ausgabe 2011/07), 146 – Oetz (Ausgabe 2011/07), Geologische Bundesanstalt, Wien.

Golas, B., 1996: Der Eibseebergsturz, Eine geomorphologische Studie, Dipl. Thesis, 1-96, Univ. Innsbruck, 1996.

Haas, U., Ostermann, M., Sanders, D., Hornung, T., 2014: Quaternary sediments in the Werdenfels region (Bavaria, southern Germany). In: Kerschner, H., Krainer, K., Spötl, C. (Eds.): From the foreland to the Central Alps – Field trips to selected sites of Quaternary research in the Tyrolean and Bavarian Alps. Geozon, 18-30.

Hammer, W., 1929: Geologische Spezialkarte der Republik Österreich 1:75.000, 5146 Ötzthal. Verlag Geol. B.-A., Wien.

Heuberger, H., 1966: Gletschergeschichtliche Untersuchungen in den Zentralalpen zwischen Sellrain und Ötztal. Wiss. Alpenvereinshefte 20, 1-126, Innsbruck.

Heuberger, H., 1975: Das Ötztal. Bergstürze und alte Gletscherstände, kulturgeographische Gliederung. Innsbrucker Geograph. Stud. 2: 213-249.

Hoinkes, G., Thöni, M., 1993: Evolution of the Ötztal-Stubai, Scarl-Campo and Ulten Basement Units. In: Raumer, J.F., Neubauer, F., (Eds.): The Pre-Mesozoic Geology in the Alps, Springer, 485-494.

Ivy-Ochs, S., Heuberger, H., Kubik, P.W., Kerschner, H., Bonani, G., Frank, M., Schlüchter, C., 1998: The age of the Köfels event. Relative, 14C and cosmogenic isotope dating of an early Holocene landslide in the Central Alps (Tyrol, Austria). Zs. Gletscherkd. Glazialgeol. 34, 57-68.

Jerz, H., 1999: Nacheiszeitliche Bergstürze in den Bayerischen Alpen. Relief Boden Paläoklima, 14, 31-40.

Jerz, H., Poschinger, A. v., 1995: Neuere Ergebnisse zum Bergsturz Eibsee-Grainau. Geologica Bavarica, 99, 383-39.

Klebelsberg, R., 1951: Das Becken von Längenfeld im Ötztal. Schlern-Schriften, 77, 399-422.

Knapp, S., Mamot, P., Krautblatter, M., 2015: The mobility of rock avalanches: disintegration, entrainment and deposition – a conceptual approach. Geophysical Research Abstracts, 17, 12496.

Krautblatter, M., Verleysdonk, S., Flores-Orozco, A., Kemna, A., 2010: Temperature-calibrated imaging of seasonal changes in permafrost rock walls by quantitative electrical resistivity tomography (Zugspitze, German/Austrian Alps). Journal of Geophysical Research – Earth Surface, 115 (F02003), 1-15.

Leith, K., Hofmayer, F., Kessler, B., Krautblatter, M., 2016: Preconditioning of the Eibsee rock avalanche by deglaciation and development of critical bedrock stresses. Geophysical Research Abstracts, 18, EGU2016-18256.

Lenhardt, W., Freudenthaler, C., Lippitsch, R., Fiegweil, E., 2007: Focal-depth distribution in the Austrian Eastern Alps based on macroseismic data. Austrian Journal of Earth Sciences, 100, pp. 66–79.

Linzer, H. G., Decker, K., Peresson, H., Dell'Mour, R., Frisch, W., 2002. Balancing lateral orogenic float of the Eastern Alps. Tectonophysics, 354(3), 211-237.

Masch, L., Wenk, H.R., Preuss, E., 1985: Electron microscopy study of hyalomylonites – evidence for frictional melting in landslides. Tectonophysics, 115, 131-160.

Nasir, A., Lenhardt, W., Hintersberger, E., Decker, K., 2013: Assessing the completeness of historical and instrumental earthquake data in Austria and the surrounding areas. Austrian Journal of Earth Sciences, 106*(1)*, 90-102.

Nicolussi, K., Spötl, Ch., Thurner, A., Reimer, P., 2015: Precise radiocarbon dating of the giant Köfels landslide (Eastern Alps, Austria). Geomorphology, 243, 87-91.

Ortner, H., 2003: Cretaceous thrusting in the western part of the Northern Calcareous Alps (Austria) – evidences from synorogenic sedimentation and structural data. Mitteilungen der Österreichischen Geologischen Gesellschaft, 94, 63-77.

Ortner, H., Reiter, F., Brandner, R., 2006: Kinematics of the Inntal shear zone–sub-Tauern ramp fault system and the interpretation of the TRANSALP seismic section, Eastern Alps, Austria. Tectonophysics, 414, 241-258.

Ostermann, M., Sanders, D., Prager, C., Kramers, J., 2007: Aragonite and calcite cementation in "boulder-controlled" meteoric environments on the Fern Pass rockslide (Austria): implications for radiometric age dating of catastrophic mass movements. Facies, 53/2, 189-208.

Ostermann, M., Prager, Ch., 2014: Causes, Kinematics and Effects of major Holocene Rock Slope Failures in the lower Ötz Valley. In: Kerschner, H., Krainer, K., Spötl, Ch. (Eds.): From the foreland to the Central Alps – Field trips to selected sites of Quaternary research in the Tyrolean and Bavarian Alps. Geozon, 116-127.

Ostermann, M., Ivy-Ochs, S., Sanders, D., Prager, Ch., 2016: Multi-method (^{14}C, ^{36}Cl, ^{234}U/^{230}Th) age bracketing of the Tschirgant rockslide (Eastern Alps): Implications for numerical dating of catastrophic mass-wasting. Earth Surface Processes and Landforms, in press.

Pagliarini, L., 2008: Strukturelle Neubearbeitung des Tschirgant und Analyse der lithologisch-strukturell induzierten Massenbewegung (Tschirgant Bergsturz, Nördliche Kalkalpen, Tirol). Unpubl. MSc thesis, Univ. of Innsbruck, 90 pp.

Patzelt, G., 2012: Die Bergstürze vom Tschirgant und von Haiming, Oberinntal, Tirol. Jb. Geol. B.-A., 152, 1-4, 13-24.

Pichler, A., 1863: Zur Geognosie Tirols. II. Die vulkanischen Reste von Köfels. Jb. k. k. Gol. R.-A., 13, 591-594.

Poscher G., 1993: Neuergebnisse der Quartärforschung in Tirol. Arbeitstagung 1993 Geol. B.-A., Geologie des Oberinntaler Raumes, Schwerpunkt Blatt 144 Landeck, 7-27.

Poscher, G., Patzelt, G., 2000: Sink-hole Collapses in Soft Rocks. Felsbau, 18, 36-40.

Prager, C., 2010: Geologie, Alter und Struktur des Fernpass Bergsturzes und tiefgründige Massenbewegungen in seiner Umgebung (Tirol, Österreich). PhD-thesis, Univ. Innsbruck, 1-307.

Prager, C., Krainer, K., Seidl, V., Chwatal, W., 2006: Spatial features of Holocene Sturzstrom-deposits inferred from subsurface investigations (Fernpass rockslide, Tyrol, Austria). Geo.Alp, 3, 147-166.

Prager, C., Zangerl, C., Poscher, G., 2007: Prominent mass movements in the Tyrol (Austria): the deep-seated Tschirgant, Tumpen and Köfels rockslides. Geo.Alp, 4, 159-162.

Prager, C., Zangerl, C., Patzelt, G., Brandner, R., 2008: Age distribution of fossil landslides in the Tyrol (Austria) and its surrounding areas. Nat. Hazards Earth Syst. Sci., 8, 377-407.

Prager, C., Ivy-Ochs, S., Ostermann, M., Synal, H. A., Patzelt, G., 2009a: Geology and radiometric ^{14}C-, ^{36}Cl-and Th-/U-dating of the Fernpass rockslide (Tyrol, Austria). Geomorphology, 103/1, 93-103.

Prager, C., Zangerl, C., Nagler, T., 2009b: Geological controls on slope deformations in the Köfels rockslide area (Tyrol, Austria). Austrian J. Earth Sc., 102/2, 4-19.

Prager, C., Zangerl, C., Kerschner, H., 2012: Sedimentology and mechanics of major rock avalanches: implications from (pre-)historic Sturzstrom deposits (Tyrolean Alps, Austria). in: Eberhardt, E. et al. (eds.), Landslides and Engineered Slopes: Protecting Society through Improved Understanding, Proc. ISL NASL 2012, Banff/Canada, 895-900, Taylor & Francis.

Prager, C., Küffler, K., Brandner, R., Hopf, S., Leblhuber, P., 2016: Engineering geological surveys and new insights at the southern margin of the Norther Calcareous Alps (Imst-Haiming region, Tyrol/Austria). GeoTirol 2016, Innsbruck.

Preuss, E., 1974: Der Bimsstein von Köfels/Tirol: die Reibungsschmelze eines Bergsturzes. Jb. Vereins zum Schutze der Alpenpflanzen und -Tiere, 39, 85-95.

Purtscheller, F., 1978: Oetztaler und Stubaier Alpen. Sammlung Geolog. Führer, 53, Borntraeger.

Purtscheller, F., Pirchl, T., Sieder, G., Stingl, V., Tessadri, T., Brunner, P., Ennemoser, O., Schneider, P., 1995: Radon emanation from giant landslides of Koefels (Tyrol, Austria) and Lang Tang Himal (Nepal). Environmental Geology, 26, 32-38.

Rothmund, S., 2012: Der Bergsturz am Piburger See. unpublished Bachelor thesis, University of Innsbruck, 1-31.

Sanders, D., 2012: Talus accumulation in detachment scars of Late Holocene rock avalanches, Eastern Alps (Austria): rates and implications. Geo.Alp, 9, 82-99.

Sanders, D., Ostermann, M., Brandner, R., Prager, C., 2010: Meteoric lithification of catastrophic rockslide deposits: Diagenesis and significance. Sedimentary Geology, 223/1, 150-161.

Schmid, S.M., Fügenschuh, B., Kissling, E., Schuster R., 2004: Tectonic map and overall architecture of the Alpine orogen. Ecl. Geol. Helv. 97, 93-117.

Senarclens-Grancy, W., 1958: Zur Glazialgeologie des Oetztales und seiner Umgebung. Mitt. Geol. Ges., 49, 257-314.

Zangerl C., Eberhardt E., Perzlmaier S., 2010: Kinematic behaviour and velocity characteristics of a complex deep-seated crystalline rockslide system in relation to its interaction with a dam reservoir. Eng. Geol.,113, 11-32.